

Supporting information

Bottom-up synthesis of ion pair-bridged metal-organic framework for H⁺ conduction

*Keiichiro Maegawa,^{*a, b} Hayata Okamoto,^a Kazuhiro Hikima,^a Go Kawamura,^a Atsushi Nagai,^b and Atsunori Matsuda^{*a}*

a. Department of Electrical and Electronic Information Engineering, Toyohashi University of Technology, 1-1 Hibarigaoka, Tempaku-cho, Toyohashi, Aichi 441-8580, Japan.

b. Next-Generation Energy Systems group, Centre of Excellence ENSEMBLE3 sp. z o.o., Wolczynska 133, Warsaw 01-919, Poland.

AUTHOR INFORMATION

Corresponding Author

* Email: matsuda@ee.tut.ac.jp (Atsunori Matsuda)

* Email: Maegawa.keiichiro.pl@tut.jp (Keiichiro Maegawa)

The supplementary information includes:

Sections S1–S4

Figures S1–S8

Table S1–S2

Section S1 Synthesis and characterization methods

Synthesis of PyDC-PA linker (Figure S1): 1g of PyDC (5.98 mmol) was dissolved in a dimethyl sulfoxide (DMSO) solution and then magnetic stirred at 60°C. The 1.2 equal amount of 85% PA against PyDC was dropped slowly into the PyDC solution under magnetic stirring, then kept stirring for 15 min. The solution was slowly dropped using a pipette into the 500 ml of diethyl ether solution under stirring at vigorous speed for reprecipitation. After that, the solution is kept stirring overnight with stirring at 300 rpm, then correct the precipitation by decantation. Decantated materials were washed with diethyl ether two times for removing an exceeded amount of PA, and centrifuged. The resulted samples were dried in vacuum oven at room temperature.

Synthesis of MOFs (Figure S2): The synthesis of UiO-66 were completely according to the method reported by Wu et al.¹. The 1.678 g (7.2 mmol) of ZrCl₄ and 1.661 g (10 mmol) of terephthalic acid were dissolved in the DMF (75 mL) with sonication. HCl (5 mL) were added, then sonicate again to obtain a uniform solution. The obtained solution was added into a Teflon autoclave and heated in an oven at 80 °C for 24 h. The product was washed with DMF two times and with acetone two times, then immersed in 200 ml of acetone with stirring (200 rpm) for 24h to remove the DMF in the pores by acetone. The washed samples were corrected by centrifuge, then put it in the vacuum oven at room temperature for 1h, followed by drying in vacuum oven at 120°C for overnight. In case of the synthesis of UiO-66-PyDC and UiO-66-PyDC-PA, the method reported by Barkhordarian, et al². were used. The 233 mg (1 mmol) of ZrCl₄ and 167.2 mg (1 mmol) of PyDC or 265.11 mg (1 mmol) of PyDC-PA were dissolved in the DMF (10 mL) with sonication. HCl (10 mL) were then added, and sonicate again to obtain a uniform solution. The

obtained solution was added into a 50 ml vial and heated in an oven at 100 °C for 24 h. The sample washing and correcting process were conducted on the same method with UiO-66 synthesis.

The chemical structure of the linkers or MOFs were characterized by FT-IR (V-670 FT-IR, JASCO) using the reflection method with attenuated total reflection attachment. XRD patterns of the prepared MOFs were recorded using Ultima IV, Rigaku ($\text{CuK } \alpha$: 1.5418 Å). For the morphological characterization of the MOFs were performed by SEM (S-4800, Hitachi). The elemental analysis were conducted by EDS (Oxford UltimMax 40, Oxford Instruments) which is installed with the SEM. BET specific surface area was analyzed and calculated using TriStar II 3020, Simadzu. Raman spectroscopic analysis was performed for the prepared linker and MOFs on a NRS-4500, JASCO with green laser ($\lambda = 531.863$ nm). XPS (PHI Quantera SXM-CI, ULVAC-PHI Inc.) was used for the elemental analysis of prepared MOFs. By using AC impedance spectroscopy and an electrochemical analyzer with a frequency response analyzer (SI1260, Solartron), proton conductivities were measured at 100 mV in the frequency range of 10 MHz to 10 Hz. The powdered samples were pelletized at a pressure of 255 MPa with Teflon-coated carbon paper (TGP-H-060H; Chemix) with $\phi=13$ mm on both sides in a stainless cell for 10 min. The obtained pellet was sandwiched by the conductivity cell, then placed in a constant temperature and humidity chamber (Yamato Scientific; IG401) for controlling temperature and humidity. The temperature and humidity in the chamber were controlled and gradually changed with five-step changes of 40, 60, 80, 90, and 95%RH while maintaining a temperature at 80°C.

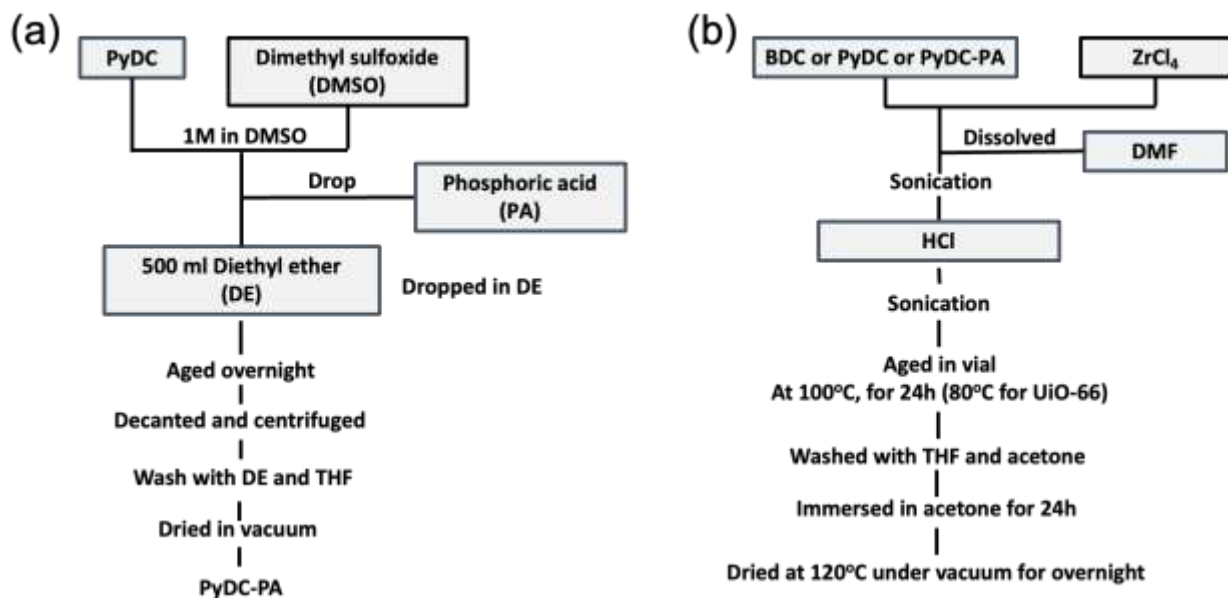
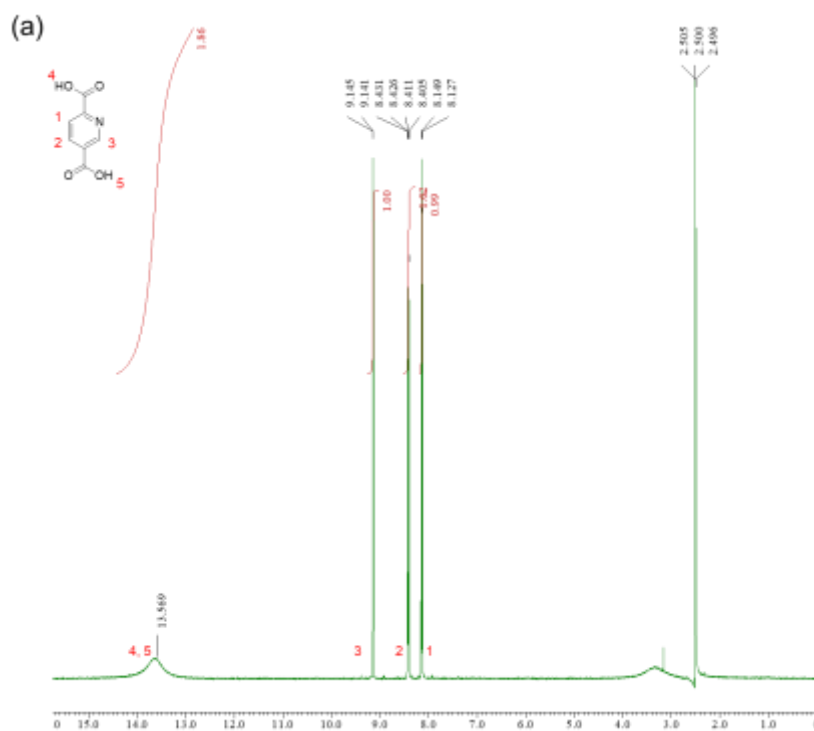
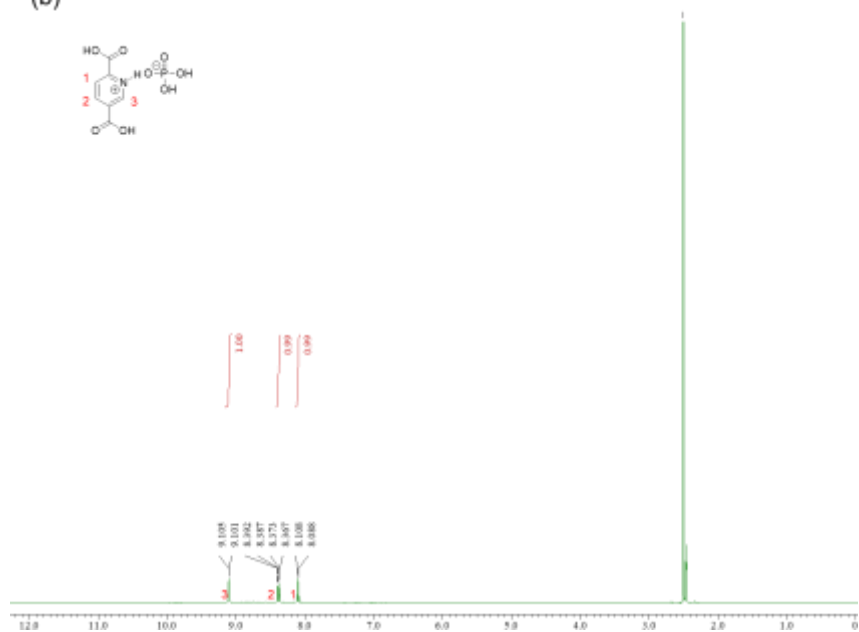


Figure S1 Experimental procedure of (a) synthesis of PyDC-PA ion pair linker and (b) synthesis of UiO-66, UiO-66-PyDC and UiO-66-PyDC-PA MOFs.

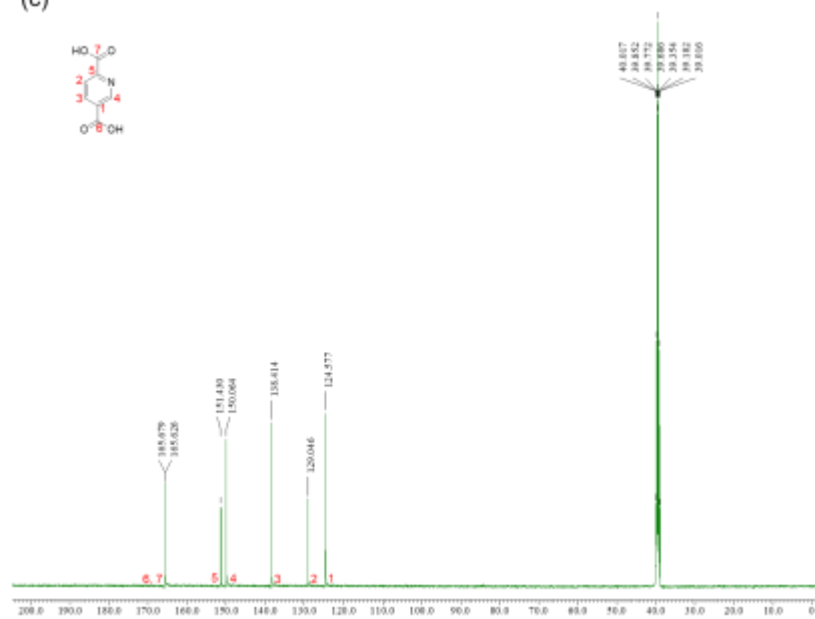
Section S2 NMR analysis and EDS elemental analysis of PyDC and PyDC-PA



(b)



(c)



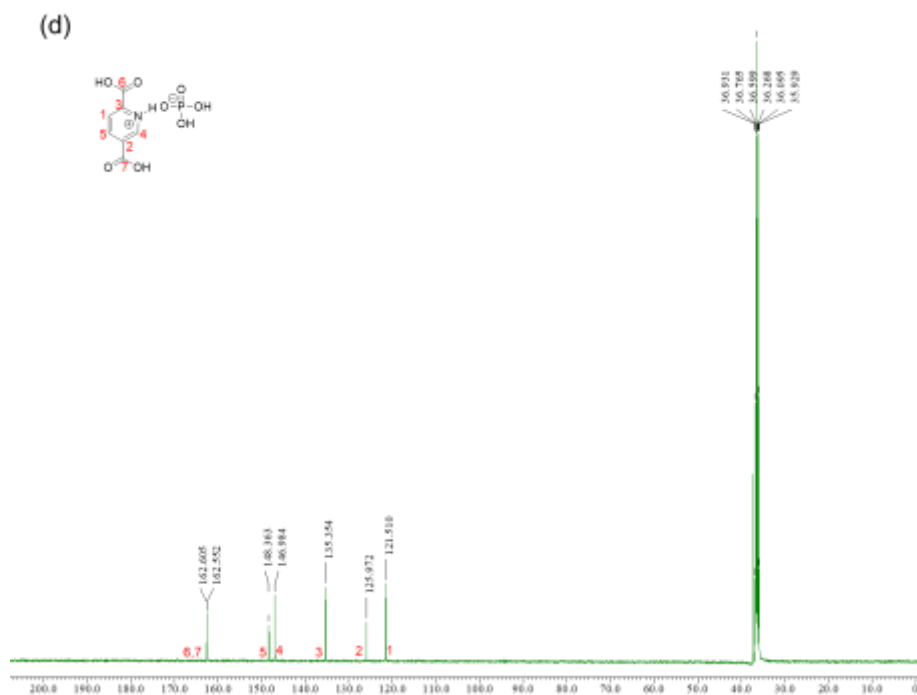


Figure S2 (a) ^1H NMR spectrum of PyDC recorded in d-DMSO, (b) ^1H NMR spectrum of PyDC-PA recorded in d-DMSO, (c) ^{13}C NMR spectrum of PyDC recorded in d-DMSO and (d) ^{13}C NMR spectrum of PyDC-PA recorded in d-DMSO.

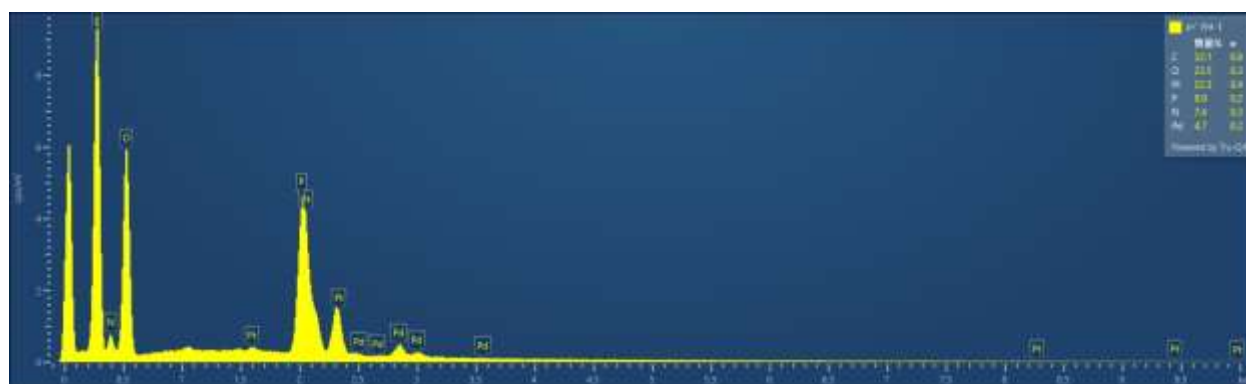


Figure S3 Spectrum of EDS elemental analysis of PyDC-PA.

Section S3 Characterization of the UiO-66, UiO-66-PyDC and UiO-66-PyDC-PA

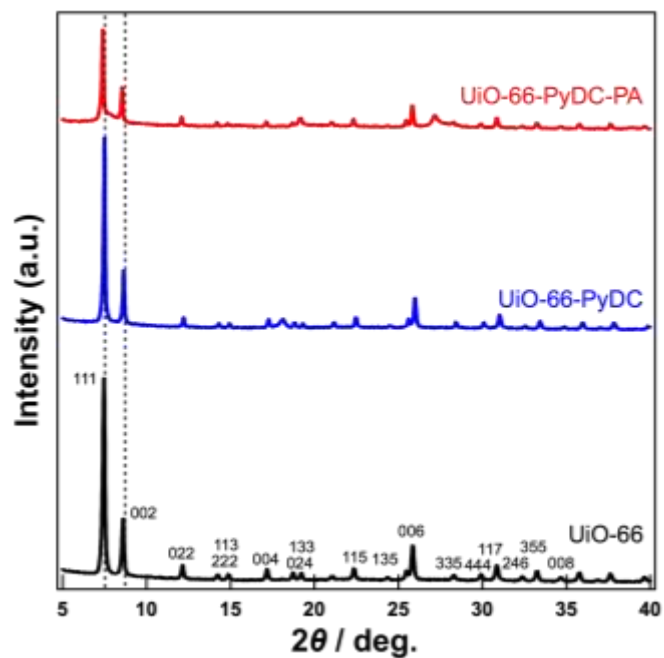


Figure S4 X-Ray Diffraction analysis of UiO-66, UiO-66-PyDC, and UiO-66-PyDC-PA in the range of 5-40°.

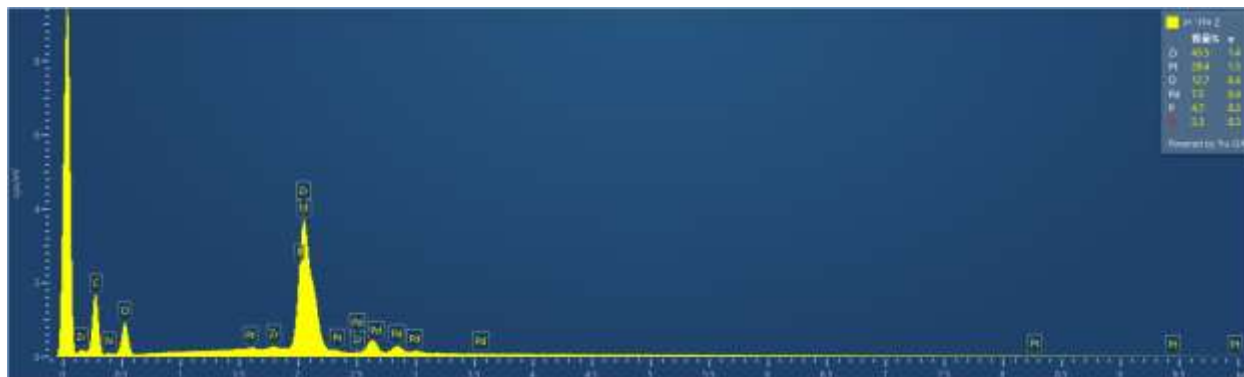


Figure S5 Spectrum of EDS elemental analysis of UiO-66-PyDC-PA.

Table S1 The result of elemental analysis obtained by XPS for UiO-66, UiO-66-PyDC and UiO-66-PyDC-PA MOFs.

Element	Atomic ratio [%]		
	UiO-66	UiO-66-PyDC	UiO-66-PyDC-PA
N	-	4.6	11.4
O	19.8	33.1	24.5
C	64.6	41.3	44.6
Zr	11.5	21.0	15.0
P	-	-	4.4
Pd	-	-	-
Pt	-	-	-

Investigation on the presence or absence of phosphate adsorption to the Zr6 node: The peaks from uncoordinated carboxylic acid groups located at around 1700-1710 cm^{-1} were investigated. As shown in Figure S6 and Figure 4(a) in the main text, the peak was not observed in all MOFs with and without PA modifications. Thus, we can conclude that there is no interaction of Zr6 nodes with both carboxylic from non-reacted linker and phosphate groups on the linkers. In addition, the intensity of broad bands around 3400 cm^{-1} is diminished when the Zr6 nodes are coordinated by the acids, according to the previous report ³. As shown in Figure S6, the weakening of bands at 3400 cm^{-1} was not observed after phosphoric acid modification, which is strong evidence that the stable immobilization of phosphate to the PyDC linker prevents binding to the Zr6 node.

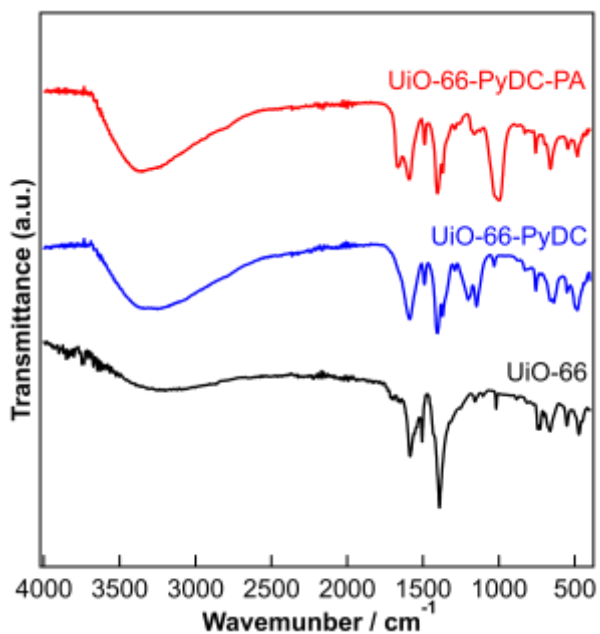


Figure S6 Full-scale FT-IR spectra for UiO-66, UiO-66-PyDC and UiO-66-PyDC-PA.

Investigation on the presence or absence of phosphate adsorption to the Zr6 node: XPS investigations were conducted to discuss the phosphoric acid adsorption on the Zr6 node, in addition to the FT-IR analysis (Figure S6). The XPS spectrum is presented in Figure S7(a). Focusing on the Zr 3d peak between 180-185 eV (Figure S7(b)), the Zr3d XPS spectra do not display any peak shifts between UiO-66-PyDC and UiO-66-PyDC-PA. The peak shifts occur when the acid groups interact with the Zr6 nodes, which is a negative phenomenon in UiO-66-PyDC-PA. Thus, we can claim that the phosphoric acid group on the PyDC-PA linker does not negatively affect the Zr6 node of the UiO-66-type MOF.

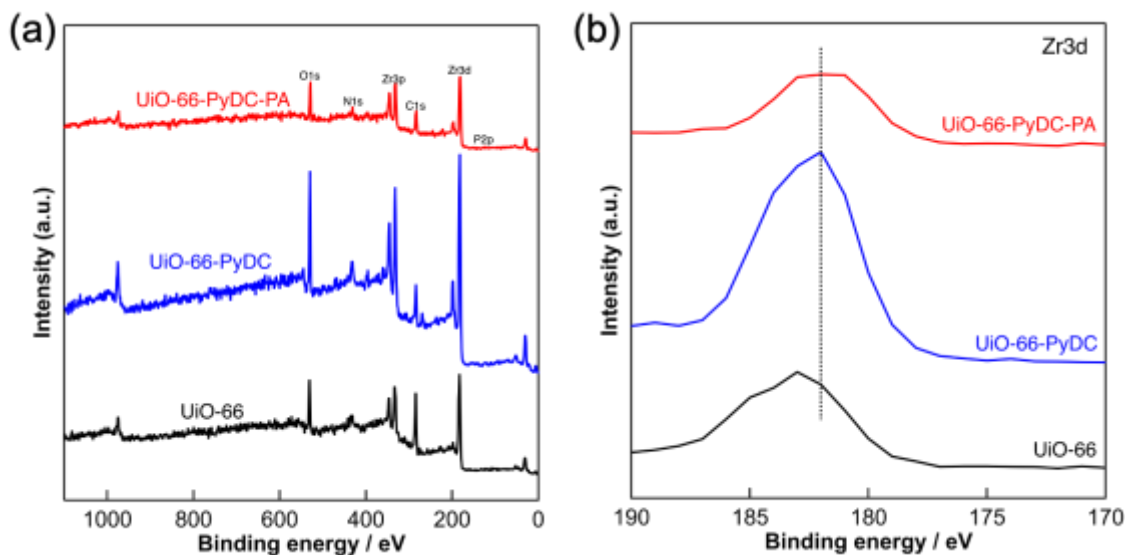


Figure S7 (a) XPS spectra for UiO-66, UiO-66-PyDC and UiO-66-PyDC-PA and (b) trimmed Zr3d XPS spectra.

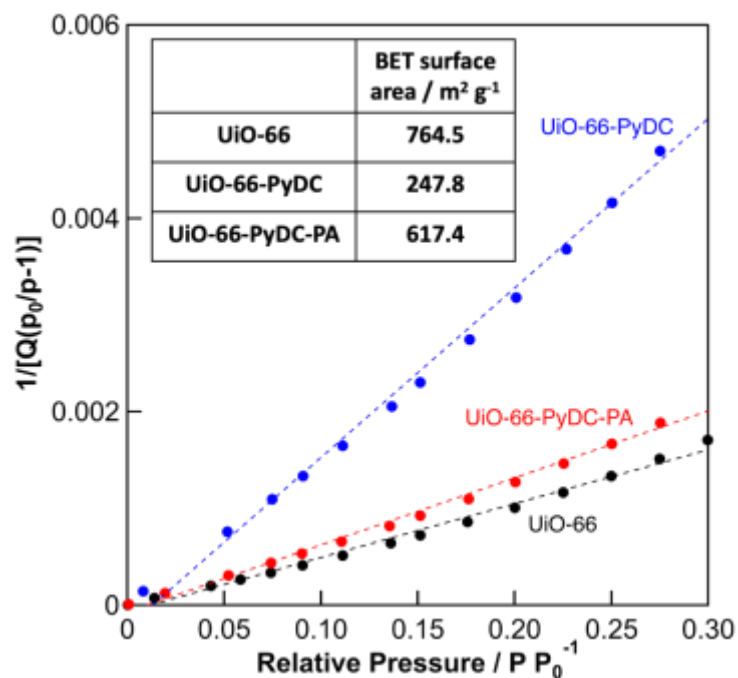


Figure S8 BET surface area plot of UiO-66, UiO-66-PyDC, UiO-66-PyDC-PA.

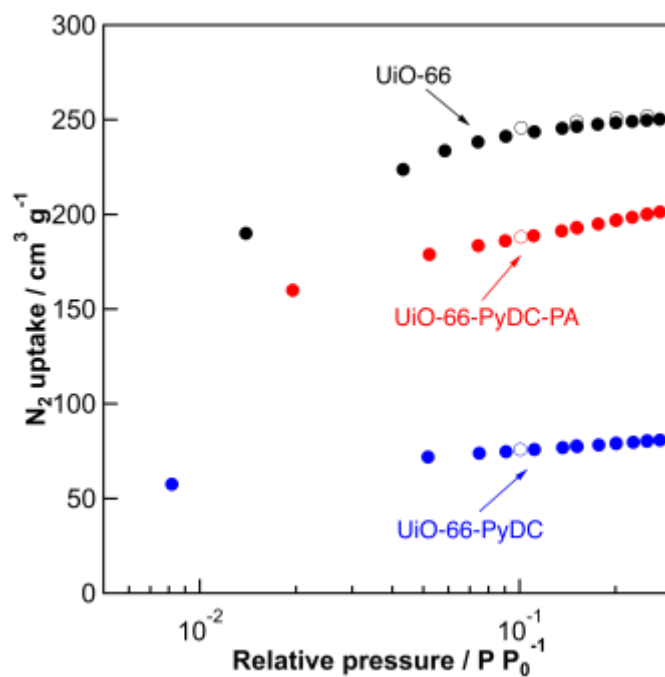


Figure S9 Semi-log graph of the low p/p_0 region of the isotherm plot for UiO-66, UiO-66-PyDC, UiO-66-PyDC-PA.

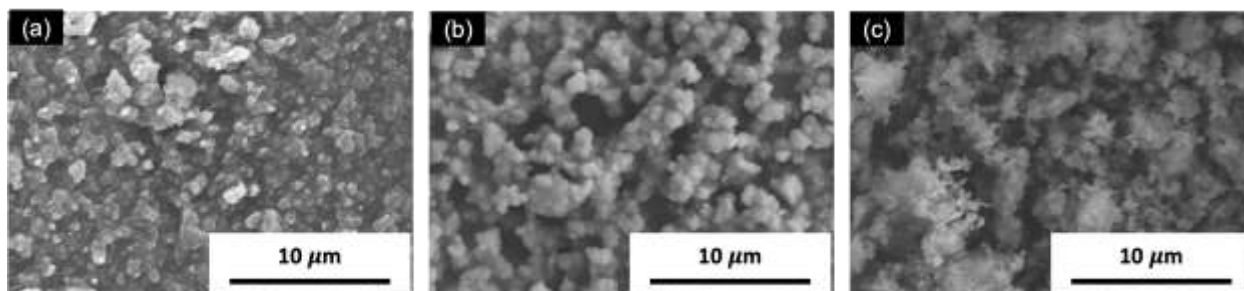


Figure S10 Morphological analysis conducted by SEM for (a) UiO-66, (b) UiO-66-PyDC and (c) UiO-66-PyDC-PA.

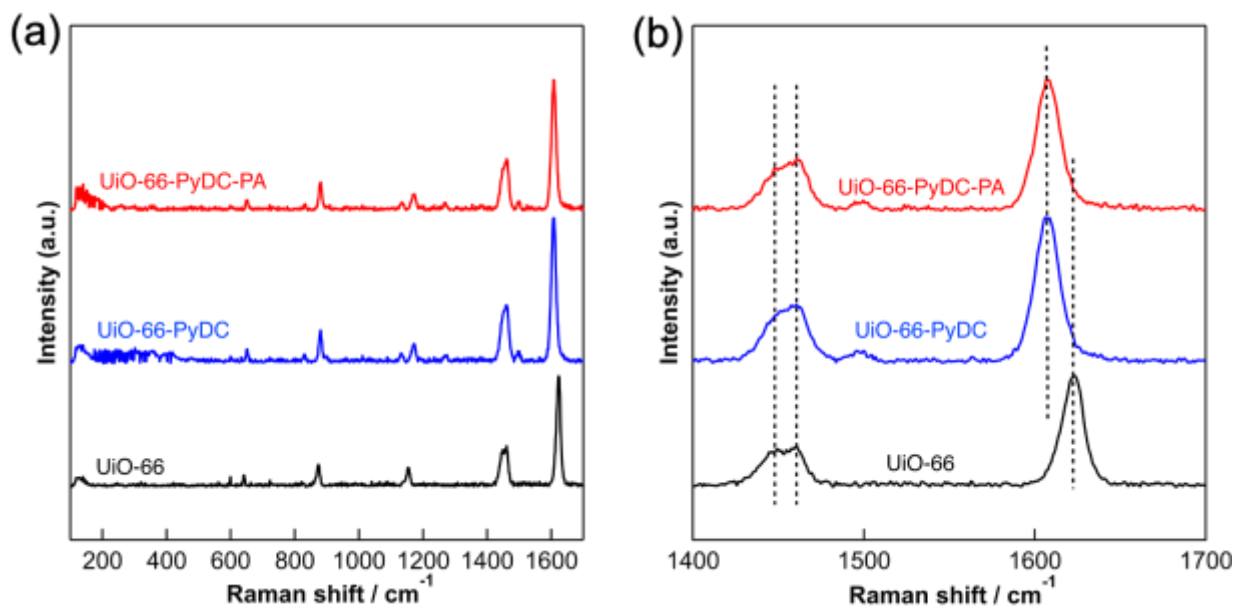


Figure S11 (a) Raman analysis for UiO-66, UiO-66-PyDC and UiO-66-PyDC-PA, and (b) their trimmed figure between 1400-1700 cm⁻¹.

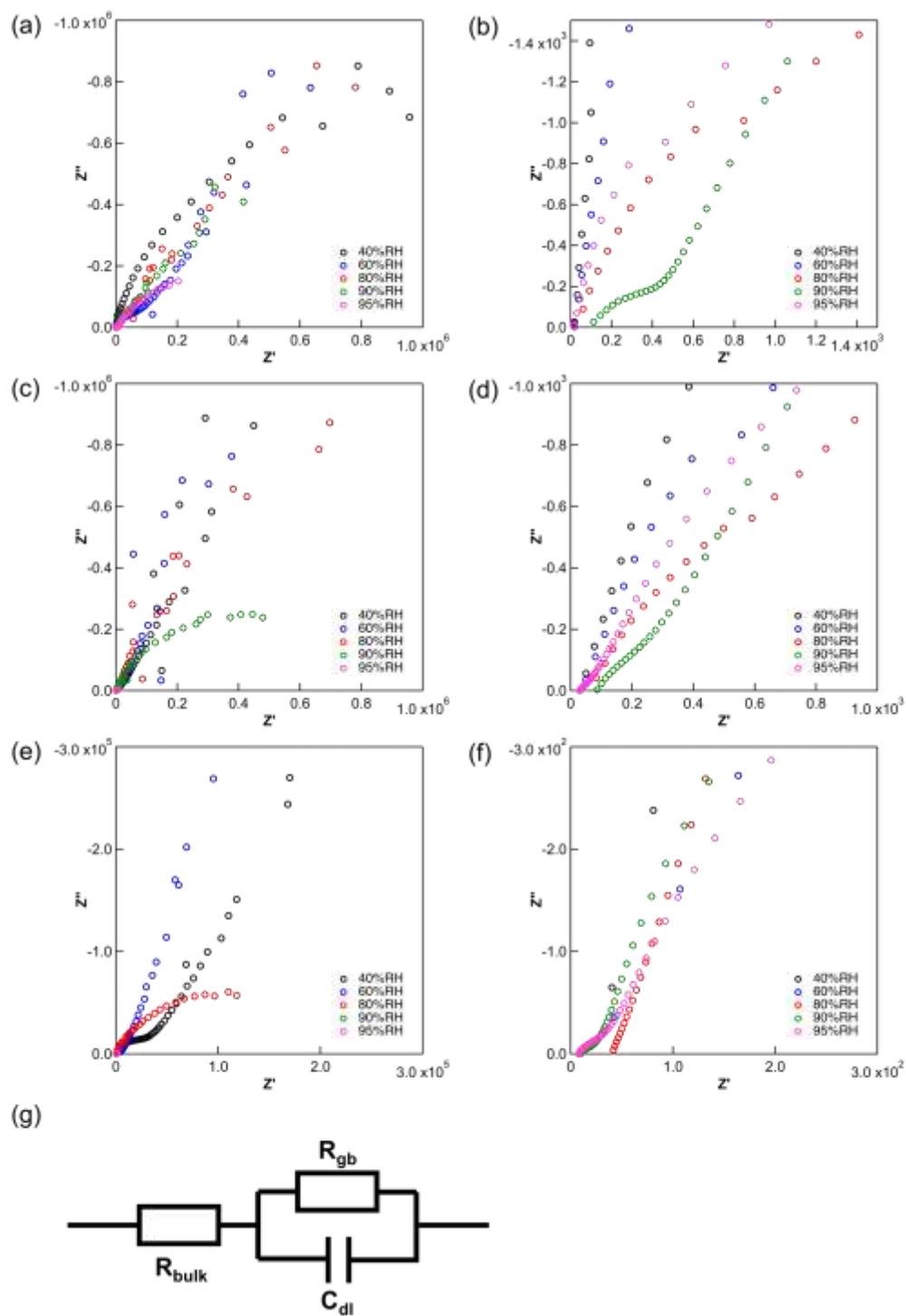


Figure S12 Nyquist plots of (a) UiO-66 (full-scale), (b) UiO-66 (trimmed), (c) UiO-66-PyDC (full-scale) (d) UiO-66-PyDC (trimmed), (e) UiO-66-PyDC-PA (full-scale) and (f) UiO-66-PyDC-PA (trimmed). (g) Equivalent circuit for the analysis.

Section S4 Structural model of the Octahedral and Tetrahedral pores of UiO-66-PyDC-PA

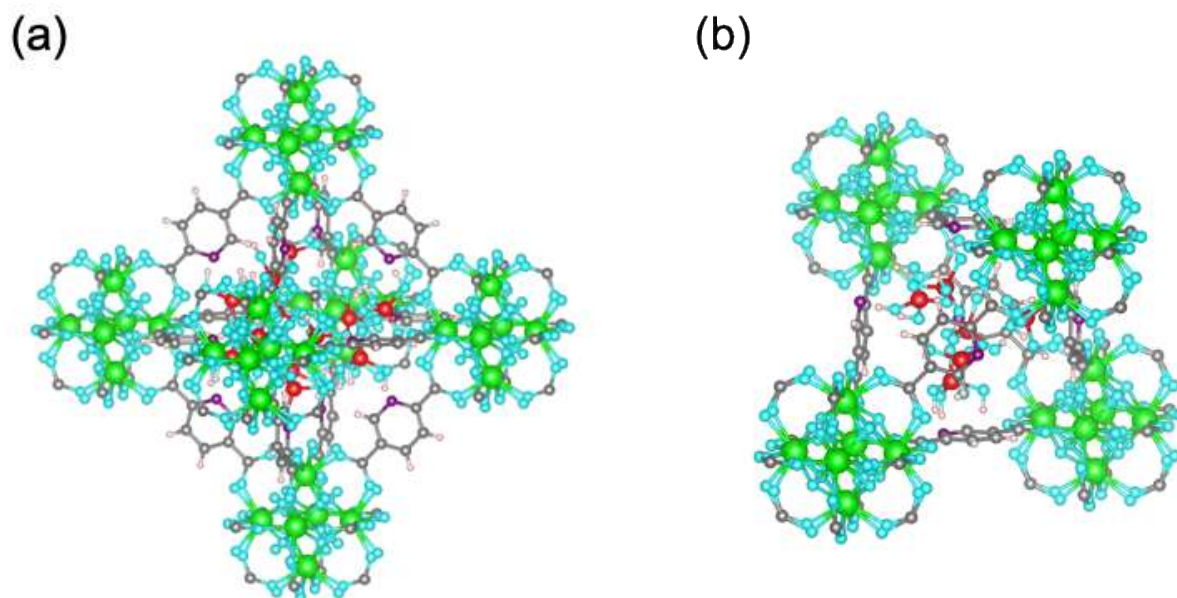


Figure S13 Structural model of the Octahedral and Tetrahedral pores of UiO-66-PyDC-PA. (a) Octahedral pore and (b) Tetrahedral pore. The crystalline structure of UiO-66 type MOF were referenced by the previously reported crystallographic file ⁴. Red: Phosphorus, Light blue: Oxygen, White: Hydrogen, Purple: Nitrogen, Gray: Carbon, Light green: Zirconium.

REFERENCES

1. Y. Wu, X. Liu, F. Yang, L. Lee Zhou, B. Yin, P. Wang and L. Wang, *Journal of Membrane Science*, 2021, **630**.
2. A. A. Barkhordarian and C. J. Kepert, *Journal of Materials Chemistry A*, 2017, **5**, 5612-5618.
3. T. Guan, X. Li, W. Fang and D. Wu, *Applied Surface Science*, 2020, **501**.
4. S. Øien, D. Wragg, H. Reinsch, S. Svelle, S. Bordiga, C. Lamberti and K. P. Lillerud, *Crystal Growth & Design*, 2014, **14**, 5370-5372.